

HEALTH MONITORING DETERIORATED CONCRETE USING AN CALORIMETRY ANALYSIS

M. Naveen Naik¹, Dr. E. Arunakanthi²

¹MTech Student (Structural Engineering), Civil Engineering Department, JNTUACEA, Anantapuramu, Andhra Pradesh, India

²Professor of Civil Engineering Department, JNTUACEA, Anantapuramu, Andhra Pradesh, India

Abstract

This project investigates the design and performance of M30 grade concrete, focusing on analysing its relations between colour profiles, deterioration and residual strength after a chemical attack using image-based techniques. The study involves casting and curing M30-grade concrete cubes over 28 days for optimal strength. After curing, the cubes were placed in four different chemical solutions: Hydrochloric Acid (HCl), Sodium chloride (NaCl), sulphuric acid (H₂SO₄), and Acetic Acid (CH₃COOH), each at a concentration of 5%. The immersion durations were 7, 14, 28, and 56 days. Following exposure, the samples undergo photography, and the images are analysed using CIE-XYZ colour space. The analysis extracts colour profiles and chromaticity diagrams to quantify the extent of chemical-induced deterioration. The results provide a detailed understanding of how different chemicals impact the structural integrity of M30-grade concrete and offer insights into the material's durability under aggressive environmental conditions. This research enhances the understanding of concrete performance in real world scenarios and contributes to improved design and maintenance practices.

Keywords: Calorimetry Analysis, Chromaticity diagrams/Image-based damage assessment, CH₃COOH, NaCl, HCl, and H₂SO₄, Residual Compressive strength.

1. Introduction

Enhancing the skeletal integrity of existing buildings is just one aspect of sustainability in construction. buildings but also addressing degradation resulting from environmental factors and aging (Ostachowicz and Güemes (2013). even while concrete constructions offer numerous benefits, they are prone to substantial deterioration when subjected to chemicals or high humidity. Understanding how different factors affect both mechanical performance and durability is essential for deciphering the intricate patterns of degradation

Digital image processing is one non-contact, non-destructive evaluation technique that has many advantages over manual measurements and visual inspections. particularly in terms of accuracy and objectivity. Digital image processing integrates various techniques and resources for gathering certain data, such as crack characteristics (such as width and length),

the spacing between microscopic gaps, the direction of the fibres in fiber-reinforced building materials, and colour changes brought on by changes in temperature, damage from fire, or chemical exposure. According to Jurevicius et al. (2014), the fundamental idea behind digital image processing is to visualise the dispersion of the relationship matrix of digital pictures in order to measure surface roughness characteristics. A further way to understand changes in compact and strength is to analyse the shape of air holes in concrete reinforced with cast iron fibres. Reported by Redon, a et al. (1999), research has been done on the relationship between air spaces and fibre orientation. SKIZ, distance function, and count-dilation approaches are a few examples of methods that have been developed using methods of digital image processing to estimate the distribution of and distance among voids (Dequiedt et al., 2001).. In order to measure fracture width, automated methods for feature extraction, such as the

Automated crack parameter estimate has been made easier with the use of fly-fisher and route finder algorithms (Dare et al., 2002). Other developments include the creation of automated systems that require little operator involvement to detect fractures and track their progression (Valença et al., 2013). A bimodal grey-level distribution of intensity is usually seen in objects that stand out from their backdrop; the threshold value is derived from the smallest point of the valleys in this distribution. When the distribution of grey level intensity is not bimodal, it displays vast valleys and huge peaks (Kapur et al., 1985). It is essential to standardise image quality for digital processing; bitumen and aggregates can be distinguished using histogram analysis, although the accuracy of this method is greatly impacted by camera management and lighting (Komač'ka et al., 2019). Additionally, when taking pictures of a black target on a bright background, the adjacency effect from nearby reflectance might result in blurred borders and contrast reduction. This is especially troublesome when taking pictures of fractures against a background that is brighter. An approach that combines under- and over-extraction techniques—a low-high threshold selection methodology—has been presented as a solution to this (Yu et al., 2019). The partially automated assessment of carbonation depth has grown reliant on digital picture processing. When carbonated structures are exposed to phenolphthalein, the non-carbonated sections turn pink while the carbonated regions stay colourless, which can be used to determine the depth of deterioration. Image histograms and computerised digital image analysis (ADIA) are used to measure this depth. ADIA combines image binarization, fuzzy c-means thresholding, Kapur's method (Kapur et al., 1985), and various segmentation techniques like Otsu's thresholds (Otsu, 1979; Segura et al., 2010). Methods like the convex hull algorithm and complementary image method, as detailed in Choi, et al. (2017), can be used to measure carbonation depth with more accuracy. Monitoring the service life, determining the carbonation depth, and residual assessing variations in surface characteristics like colour and texture is necessary to determine the strength of structures. Different colour spaces are used in digital image processing, including RGB stands for red, green, and blue; HSV for hue, saturation, and lightness; HSL for hue, saturation, and lightness; CIE-XYZ for Commission Internationale de l'Éclairage-XYZ coordinate; and CIE-Lab* for Commission Internationale de l'Éclairage-LAB coordinate (Ibraheem et al., 2012). To correctly delineate damage areas and pinpoint regions of interest, the analysis usually entails applying segment through thresholding techniques, producing binary images, correcting white balance utilising colour analysers (e.g., X-Rite colour check), and converting images to

greyscale. By transforming RGB photographs of thermochromic materials into CIE-LAB colours space values and then analysing the results using MATLAB, Panák et al. (2018) have made recent advances that improve a simulation of person's vision and lightness perception.

Defining Characteristic Temperatures and Visualizing the Hysteresis Loop: Key thermal points used to investigate how materials react to temperature changes are known as characteristic temperatures. The material's properties evolve with changing temperatures, as seen by the flexible hysteresis loop that is formed from these temperatures.

Colour Fidelity and Image Transfer: Colour fidelity must be guaranteed in order to process and analyse images on various systems and devices. Generally, RGB values are transformed to CIE-XYZ values during image transfers to preserve colour integrity. Look-up tables and polynomial transformations can be used for this conversion, as explained by Cheung et al. (2004). Plotting the colour changes of concrete in reaction to heat over predetermined periods of time on a colour diagram is a crucial tool for assessing the material's resistance to fire damage. Wei et al.'s (2019) description of this technique provides insightful information on how concrete handles heat exposure and evaluates its fire resistance.

According to Mackechnie and Alexander (2009), assessing the durability of construction materials is a crucial aspect of life cycle evaluation in order to guarantee their long-term sustainability. Concrete can deteriorate chemically, physically, and mechanically, among other ways that might shorten its shelf life (Press, 2007). Several models and techniques have been developed to evaluate the durability of concrete. According to Basheer et al. (2001), they are centred on comprehending how various transport processes inside the concrete impact its durability, which is frequently assessed using metrics like absorption, permeability, and diffusion. Under a study to evaluate the acid endurance of regular concrete, histogram analysis was used to analyse degradation after exposure to several chemicals under moderately bright indoor (MLI) settings. The mean compression strength of concrete samples was compared with the corresponding greyscale intensities after 3, 7, 28, and 56 days of submerge using correlation graphs. Results showed that there was a significant association between black and white intensity and degradation of concrete and strength loss for both the acid hydrochloric (HCl) and acetate (CH₃COOH). But for sodium chloride (NaCl) and sulphuric acid (H₂SO₄), this link proved less reliable (Guru Prathap Reddy et al., 2020).

2. Research Significance

Accurately estimating a major infrastructure element's remaining service life becomes more crucial when it approaches its "critical age," which includes bridges, dams, above reservoirs, and heritage structures. To comprehend the intricate patterns of degradation brought about by different environmental conditions, it is imperative to evaluate the relationship between a structure's durability and mechanical performance. Through the use of digital image processing tools, this study attempts to analyse and correlate the declines in concrete's physical performance and durability caused by environmental degradation. To be more precise, colorimetry analysis was used to lessen the subjectivity that comes with visual examinations. The purpose of the study is to determine a relationship between the concrete's remaining strength and durability and the extent of deterioration, as shown by modifications to the colour profiles of impacted surfaces.

3. Material

30 MPa typical strength concrete was employed in this investigation. The ingredients were chosen and proportioned: cement, water, coarse aggregate, and fine aggregate. in accordance with the guidelines specified in the Indian Standard Codes IS:12269-2013, IS:383-2016, IS:10500-2012, and IS:10262-2019 (BIS, 2019), as detailed in Tables 1 and 2. Table 1 describes the processes used in IS:516-2018 (BIS, 2018) for the casting and testing of concrete cubes with dimensions of 150 x 150 x 150 mm.

4. Experimental Method

Each of the four acids—hydrochloric, sulphuric, acetic, and sodium chloride—was added to an aggregate of 54 concrete squares in order to assess how well they performed mechanically and through time. These settings were applied to the cubes for seven, fourteen, twenty-eight, and fifty-six days of exposure.

After curing for 28 days, the specimens underwent compressive strength testing to determine baseline values for further study. Concrete samples immersed in specific reagent solutions were then subjected to compressive strength testing under a constant loading rate, in accordance with the procedures detailed in Indian Standard IS:516-2018.

Table 1. Materials Utilized for Sample Preparation

Materials	Specification	Standard Code
Cement	Ordinary Portland Cement, Grade 53	IS:12269-2013
Fine Aggregate	Zone-II River Sand, Machine Crushed	IS:383-2016
Coarse Aggregate	Granite	IS:383-2016
Water	Potable	IS:10500-2012

Table 2. Mix proportions (obtained as per IS:10262-2019)

Material	Weight (Kg/m ³)
Cement	448
Water	197
Fine Aggregate	742.69
Coarse Aggregate	1016.56
Water/Cement Ratio	0.44

Colourimetry analysis

To monitor alterations to the samples' colour profile exposed to reagent solutions for 7, 14, 28, and 56 days, various colour models can be employed. The RGB colour space, widely used for analyzing According to Hager (2014), the colour profiles of damaged surfaces use a three-dimensional (3D) coordinate structure in which the intensity of colour is represented by particular red, green, and blue values, each ranging from 0 to 255. 255 represents white in this model, whereas 0 represents black. However, using a single-dimensional (2D) coordinate system to visualise the RGB histogram may result in negative values due to its 3D nature. Additionally, RGB-based histogram analysis is limited by its device-dependence, which means that colour information can vary based on the device used to view the image, complicating replication and standardization for future use.

In contrast, the CIE-XYZ colour space is a device-independent 2D coordinate system (Colombo and Felicetti, 2007). This model allows for standardized and easily replicable chromaticity-based analysis employing RGB-derived CIE-XYZ values data, making it more suitable for

consistent image processing tasks. The CIE-XYZ model aligns more closely with human visual perception. Conversion from Both neural networks and polynomial transformations can be used to convert the RGB colours to CIE-XYZ values. often preferred for their accuracy and simplicity. In this model, the X and Y components provide colour information, while the Z component represents luminance. Since lighting conditions generally affect brightness rather than colour, colour analysis remains reliable across different lighting scenarios.

By plotting for every kind of attack, an acid-based, salt-based, and sulfate relative to immersion duration, we can gain insights into colour shift trends. Analyzing these trends in relation to reductions in strength or specific durability factors can help elucidate the connection between durability performance and visual colour changes. This understanding could facilitate the development of an image-based model for detecting deterioration.

5. Experimental setup

For image acquisition, three lighting conditions were tested: Lights that are bright outside (OBL), medium inside (MLI), and dim inside (ALI). After assessing the variations in greyscale values under these conditions, MLI was chosen as the standard for this study due to its consistency. Images of all six faces of After submersion, cubes that were both damaged and undamaged were taken for 7, 14, 28, and 56 days under the MLI condition.

The colour equilibrium of the was adjusted using a color-checker card. images. This calibration process corrects the colour information in the images, ensuring accuracy for subsequent analysis (see Figure 1). After calibration, the images were organized based on the type of reagent and immersion duration.

6. Analysis and discussions

'ImageJ,' an open-source Java-based image processing program frequently employed for healthcare images, particularly 3D live-cell scanning and radiological analysis, was used to analyse calibrated pictures. as well as in digital image processing studies in civil engineering. Visualising the degree of degradation for each immersion duration was made possible by this software. (7, 14, 28, and 56 days) and the generation of corresponding 3D surface maps.

Every concrete cube's six faces were analysed, calibrated, and inspected for damage. The concrete's worst-affected faces are shown in Figures 2–5. cubes exposed to various acids over specified immersion durations. Figure 2 shows the damage from hydrochloric acid exposure, with

calibrated surface graphs showing a discernible shift in the direction of red. Figure 3 illustrates how exposure to sulphuric acid causes degradation that is typified by the development of ettringite as a result of the acid's reaction with calcium hydroxides, which causes a tendency for the images to shift white. Figures 4 and 5 show how magnesium sulphate and sodium chloride, respectively, cause early discolouration and the development of white spots. are observed. However, the colour changes for these exposures over subsequent durations were less pronounced.

Development of chromaticity diagram

To convert visual superior colour changes into quantitative data, RGB values of pixels showing deterioration are translated into CIE-XYZ values. In the The Z component of the CIE-XYZ colour system denotes brightness. rather than colour information. Consequently, Colour details can be accurately represented in the XY plane with the Z component set to 0, mirroring the hue shown in the picture (refer to Figure 6). According to Wei et al. (2019), changes in the amount of light will have an impact on the plane's level yet not the colour. By charting the coordinates for x and y that were obtained using the CIE-XYZ values on a 2D graph, we can numerically represent colour information effectively. This process is conducted after selecting the concrete face for analysis.



Figure 1. (a) Uncalibrated control sample; (b) calibrated undamaged control sample; (c) calibrated damaged Sample

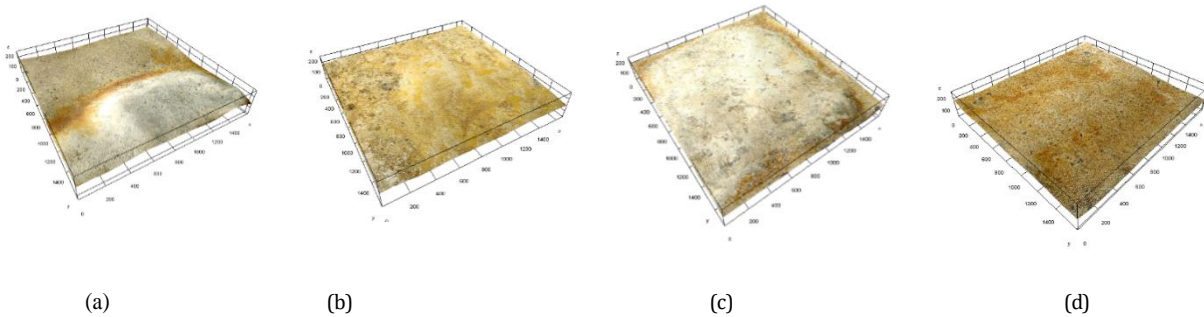


Figure 2: Surface deterioration due to immersion in a 5% hydrochloric acid solution was analyzed through 3D surface plots over various time intervals. The plots illustrate the extent of surface degradation after (a) 7 days, (b) 14 days, (c) 28 days, and (d) 56 days of exposure.

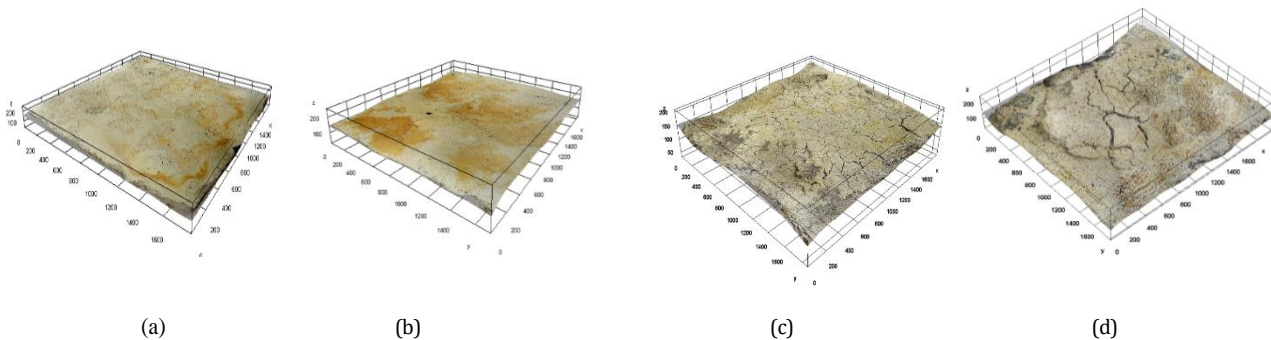


Figure 3: 3D surface plots depicting the deterioration of surfaces due to immersion in a 5% sulfuric acid (H_2SO_4) solution are shown for the following exposure periods: (a) 7 days, (b) 14 days, (c) 28 days, and (d) 56 days.

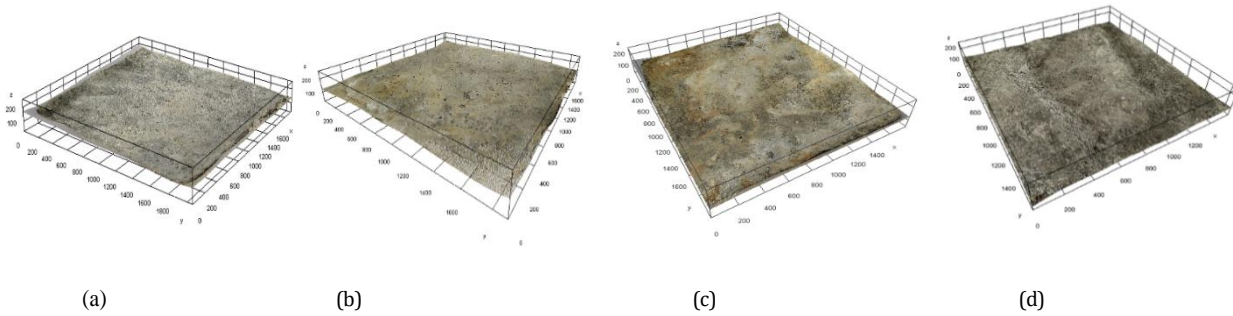


Figure 4: 3D surface plots depicting the surface deterioration resulting from immersion in a 5% sodium chloride (NaCl) solution are presented for the following time intervals: (a) 7 days, (b) 14 days, (c) 28 days, and (d) 56 days.

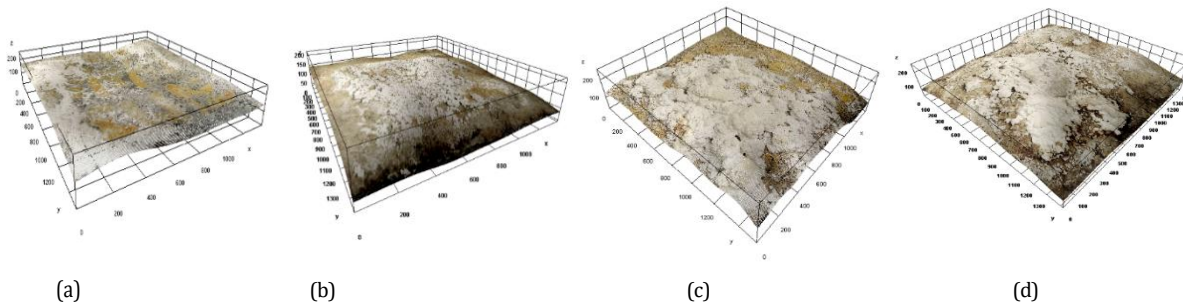


Figure 5: 3D surface plots showing the deterioration of surfaces due to CH_3COOH , Acetic acid immersion at a 5% concentration after: (a) 7 days, (b) 14 days, (c) 28 days, and (d) 56 days.

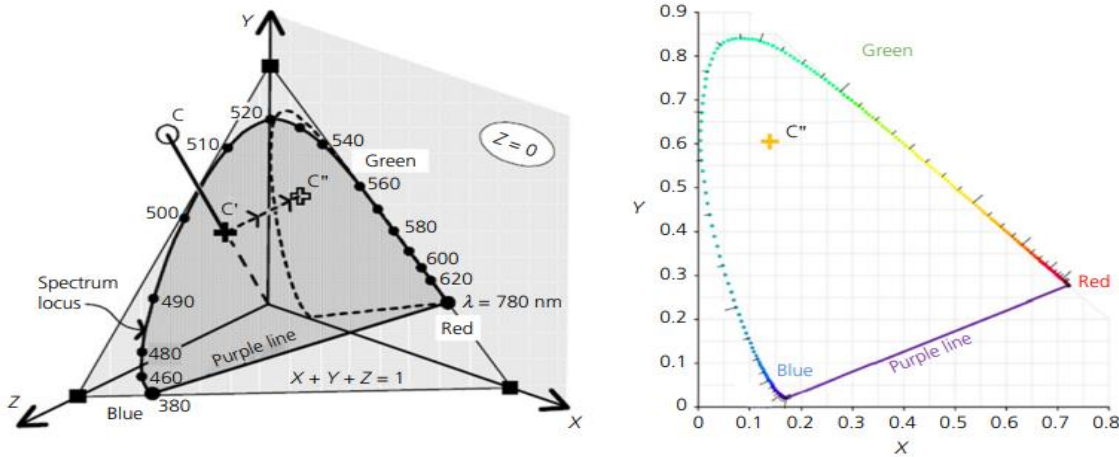


Figure 6. Chromaticity diagram (Wei *et al.*, 2019)

The RGB colour channels are exhibiting significant degradation, necessitating a transformation to convert pixel RGB values into CIE-XYZ colour space. This involves

applying polynomial transformations to map the RGB intensities to CIE-XYZ values that correlate with them. Subsequently, The chromaticity diagram is able to

generated based on these transformed values. The process for generating a chromaticity diagram involves the following steps:

(a) Extracting RGB Data: Start by gathering the image shows the deteriorating concrete surface's RGB colour information. This is a process that takes selected pixels and averages their RGB values to accurately depict the image's colour profile.

(b) Conversion to XYZ Colour Space: Convert the RGB values into the Polynomial changes in XYZ colour space, as described by Cowan (1983).

1. $X = 0.41245.R + 0.35758.G + 0.18042.B$
2. $Y = 0.21267.R + 0.71516.G + 0.07217.B$
3. $Z = 0.01933.R + 0.11919.G + 0.95023.B$

where the RGB colour space's colour coordinates are represented by R, G, and B.

(c) By normalising and projecting the XYZ values into the X-Y plane (Z=0), the impact of light intensity is reduced. We next use the following formulas to obtain the chromaticity coordinates, x and y:

4. $x = X/(X + Y + Z)$
5. $y = Y/(X + Y + Z)$

Finding the pixels that most accurately captured the colour features of the damaged surface was the main goal. In order to do this, many techniques for choosing the ROI (region of interest) were assessed. It was assumed that the chosen pixels within these regions would accurately capture the overall colour information of the damaged area. For this study, both rectangular and random pixel-based ROIs were used, depending on the specific requirements (refer to Figure 7).



Figure 7. (a) Rectangular region of interest selection; (b) random pixel selection

Rectangular and polygonal regions of interest (ROIs) encompass a large number of pixels, enabling accurate determination of the mode values from the RGB color histograms. These mode values correspond to the most frequently occurring RGB values within the ROI. In contrast, the random pixel selection method involves fewer pixels, leading to less reliable mode values. Therefore, for random pixel selections, 'The RGB histograms' mean values were utilised in their place. That was discovered. the differences between the mode values derived from the rectangular and polygonal ROIs and the mean values obtained from the random pixel selections were minimal across all images analyzed. As a result, mode values from the RGB histograms of rectangular and/or polygonal ROIs were used for the primary analysis, while mean values from random pixel selections served for validation.

To increase accuracy, For cross-validation, RGB values from two or three of the cube's less damaged faces were examined alongside those from the face that had suffered the most degradation. After selecting pixels from the calibrated images, the x and y chromaticity coordinates were calculated based on their immersion durations, following the methods described in Procedures (b) and (c). Next, the chromaticity diagrams corresponding to these values were created.

7. Results and Discussion

Examination of Chromaticity Diagrams

Chromaticity graphs for samples submerged in the corresponding solutions were created after that. we analyzed the colour profile changes across samples for each solution over specific immersion periods. This analysis also included evaluating the colour variations between samples that were submerged for a set amount of time in various solutions.

During the examination for samples submerged in hydrochloric acid in terms of x and y values, we identified several outliers that deviated significantly from the typical x and y values for that particular immersion duration. These outliers likely indicated localized damage caused by hydrochloric acid rather than reflecting the overall colour of the damaged surface. Consequently, these data points were excluded from further analysis.

Plotting the remaining information points on the chromaticity graph, as shown in Figure 8, showed a clear shift towards red, which was especially apparent when comparing the data points after 14 days of immersion in hydrochloric acid with the control sample. Visual

inspections corroborate this shift, showing significant alterations in The 3D area plots depicted in Figure 2 show the deteriorated surfaces after exposure to hydrochloric acid for 7 and 14 days.

Additionally, the data from the 14-day hydrochloric

acid immersion point suggests a white shift, as shown by a shift to the origin, in comparison to the data points from the 28-day immersion in hydrochloric acid, as shown in Figure 2. Significant inconsistencies in the data were observed after 14 days of hydrochloric acid exposure and again at the 56-day mark, with a pronounced a red colour profile that appears on the inside of the concrete cube.

The subsequent analysis adhered to a similar approach. When evaluating data points from samples exposed to sulfuric acid, a notable inconsistency emerged after 14 days of immersion. The colour data, which indicated maximum deterioration, might not always reflect accurate conditions. The surface showing inconsistent values likely provided erroneous colour information, possibly due to sulfuric acid reacting with surface impurities.

After being submerged in sulphuric acid for 14 days, there was a noticeable change in the data points' location from the origin, as seen by a chromaticity graph. As illustrated in Figure 9, there was a discernible trend into the colour white when compared data points from the 56-day soaking period with those from the control sample. Figure 3 displays 3D surfaces plots of the damaged surfaces at several time periods (7, 14, 28, or 56 days), which support this observation. Notably, samples immersed for 28 days displayed considerable surface pop-outs. When these surfaces break down and the formation of white salts, such as ettringite, contributed to the white shift observed in the chromaticity diagram.

The chromaticity graphs for the samples are shown in Figures 10 and 11. immersed in sodium chloride and acetic acid, respectively. The data show minimal variations in colour profiles across different immersion periods, suggesting limited changes in surface colour over time for these reagents. Consequently, any localized colour changes should be regarded as specific points of interest, as the

overall colour profile of samples exposed to sodium chloride and acetic acid did not exhibit significant shifts due to their slow reactivity.

In both diagrams, the data points show a change from the starting point to the 28-day immersion period. This shift is attributed to the initial absorption of the reagents, followed by a saturation point and the gradual reactivity of sodium chloride and acetic acid. For samples exposed to sodium chloride, The 28- and 56-day data points show a discernible movement in favour of white. The 3D surfaces plots in Figure 4 that depict the emergence of white spots on the destroyed samples as a result of calcium hydroxide leaching are consistent with this observation. caused by sodium chloride exposure.

For samples immersed in acetic acid the chromaticity graph barely slightly shifts towards white at the 28 and 56-day data points. Specifically, the 56-day data point is positioned near the red end of the spectrum, with only a slight shift towards white compared to the 7-day immersion point. The colour change profiles are depicted in Figure 5. To further understand the variations in colour profiles observed on deteriorated surfaces, additional analysis was performed to assess the effects of each deteriorating agent.

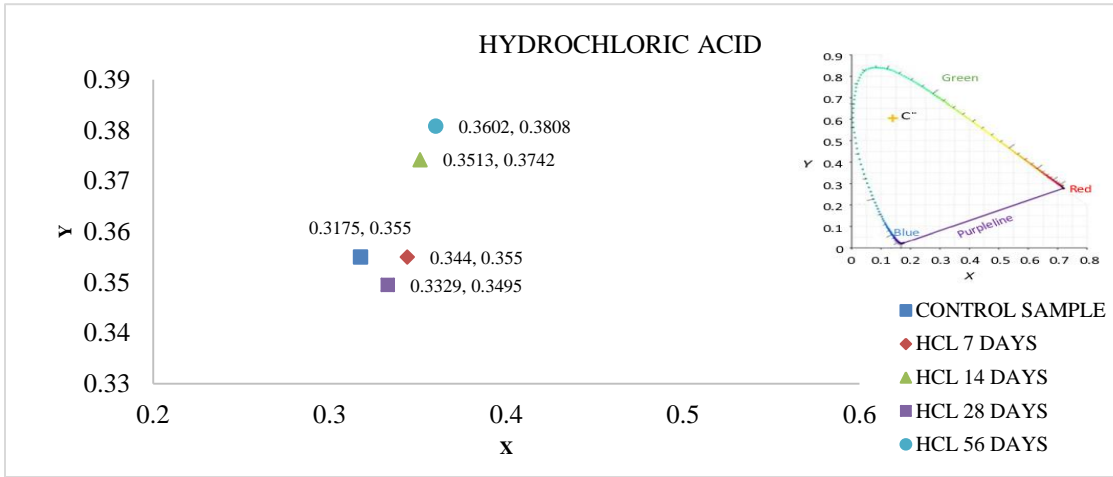


Figure 8: Chromaticity diagrams showing (a) the control sample and the surface deterioration resulting from immersion in a 5% hydrochloric acid (HCl) solution after (b) 7 days, (c) 14 days, (d) 28 days, and (e) 56 days.

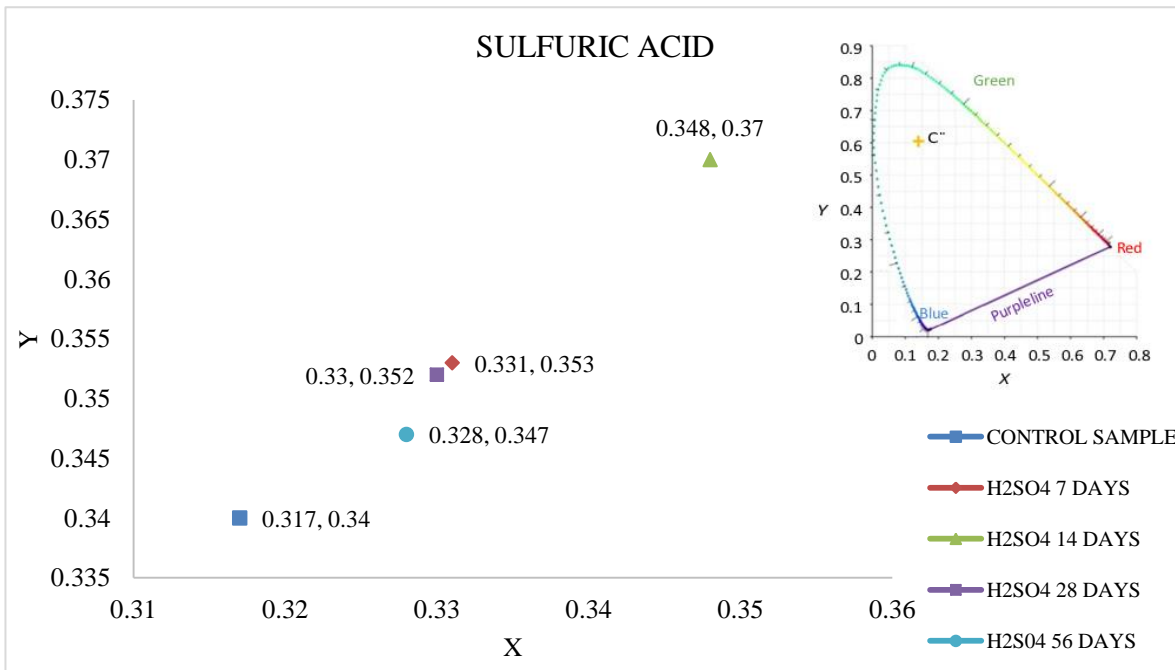


Figure 9: Chromaticity diagrams illustrating (a) the control sample and the surface degradation resulting from immersion in a 5% sulfuric acid (H₂SO₄) solution after (b) 7 days, (c) 14 days, (d) 28 days, and (e) 56 days.

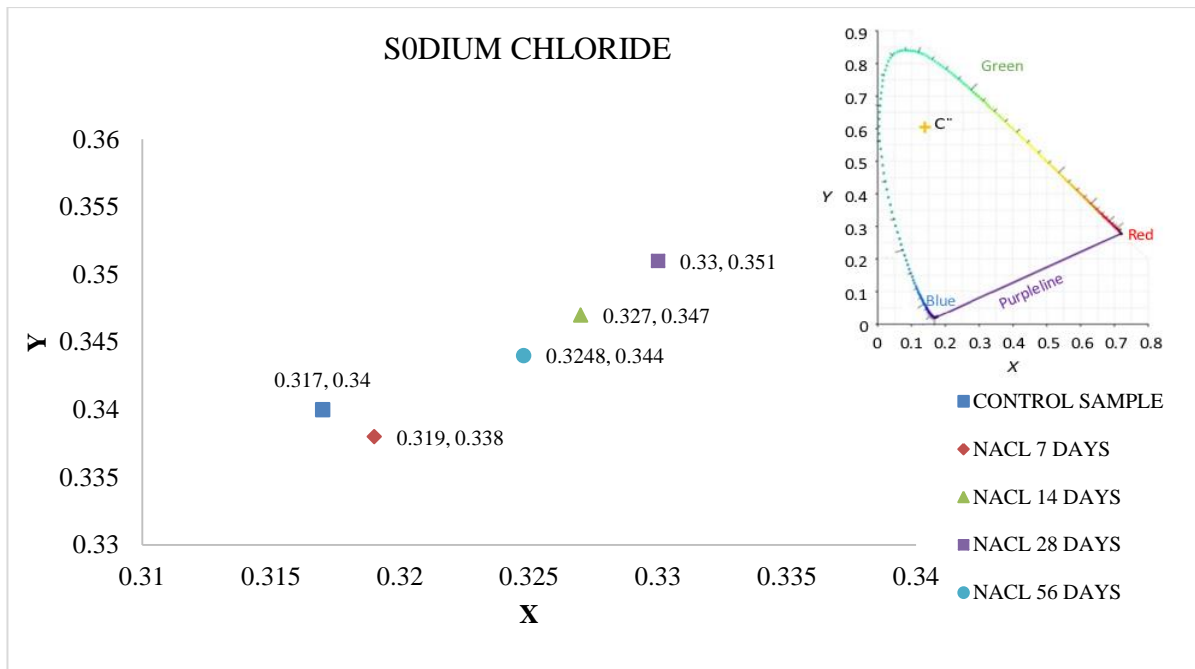


Figure 10: Chromaticity diagrams depicting (a) the control sample and the surface degradation from immersion in a 5% sodium chloride (NaCl) solution after (b) 7 days, (c) 14 days, (d) 28 days, and (e) 56 days.

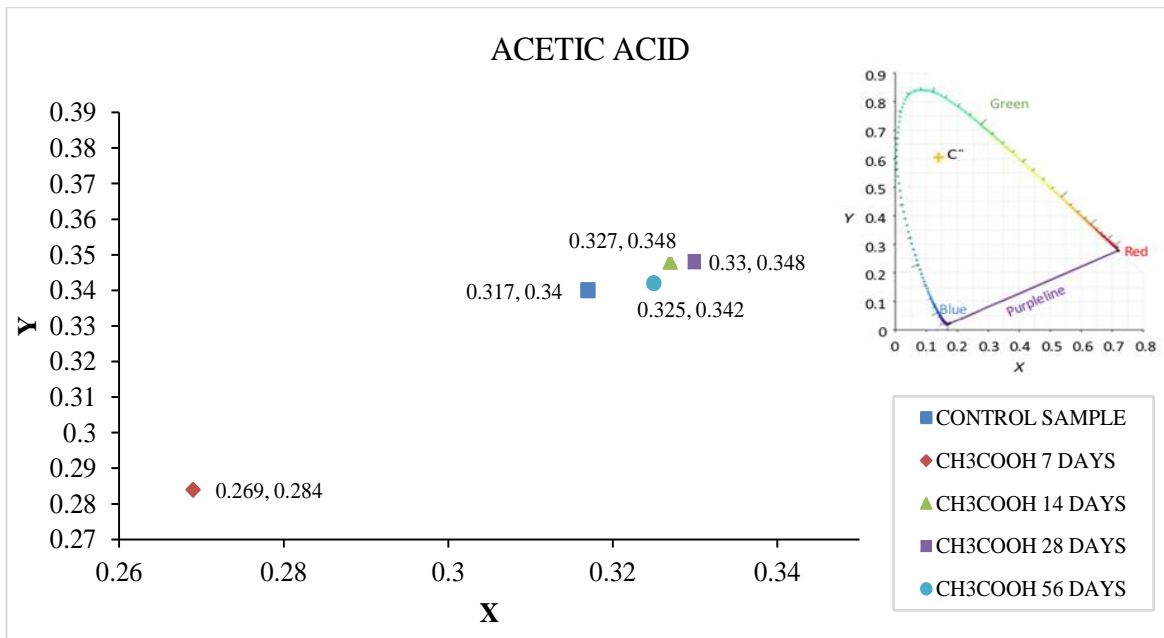


Figure 11: Chromaticity diagrams illustrating (a) the control sample and the deterioration of surfaces following immersion in a 5% acetic acid (CH₃COOH) solution for (b) 7 days, (c) 14 days, (d) 28 days, and (e) 56 days.

Hydrochloric acid, sulfuric acid, sodium chloride, and acetic acid were employed for specific durations in this study. The objective was to assess whether the chromaticity coordinates of samples immersed in these chemicals for the specified time periods could effectively differentiate the types of damage inflicted by each substance.

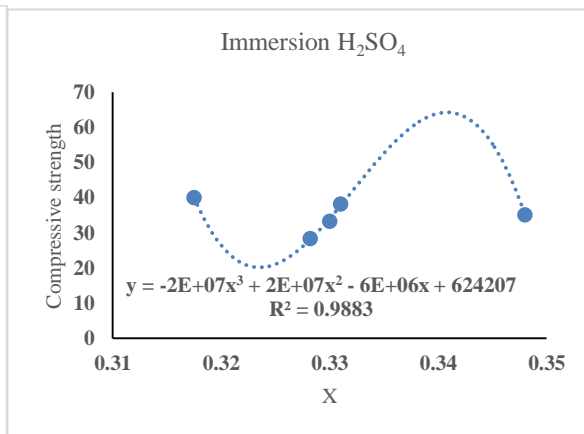
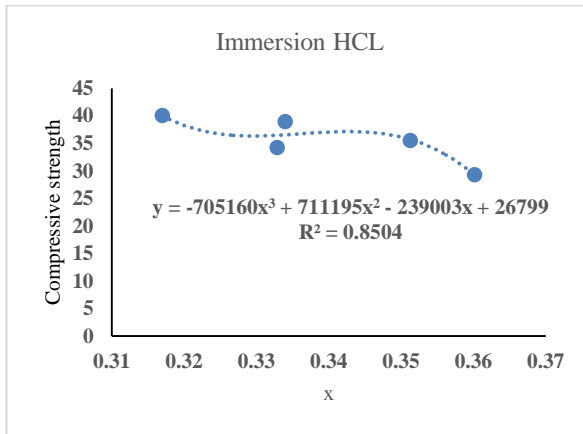
Table 3. Compressive Strengths of Samples and Control Cubes After Immersion in Various Solutions for Certain Lengths of Time The reduction in compressive strength observed after immersion in sulfuric acid is significantly greater than that caused by hydrochloric acid, with a 5%

greater reduction in strength compared to hydrochloric acid exposure.

Figure: 12 presents the polynomial relationships relationship with the colour 'x' values with the associated compressive strength values of the samples over different immersion periods (7, 14, 28, and 56 days). The analysis indicates that while the correlations between chromaticity 'x' values and compressive strength show similar trends across various immersion conditions, the slope of these relationships differs based on the reactivity of the reagent used.

Compressive Strength: MPa Table 3. Residual Compressive Strength (MPa) for Various Chemicals and Immersion Durations

Immersion Duration: Days	Control cube	HCL	H ₂ SO ₄	NaCl	CH ₃ COOH
0	0	0	0	0	0
7	40.02	38.92	38.21	39.92	39.81
14	40.02	35.47	35.12	39.13	39.15
28	40.02	34.17	33.24	38.25	37.93
56	40.02	29.23	28.35	37.52	36.67



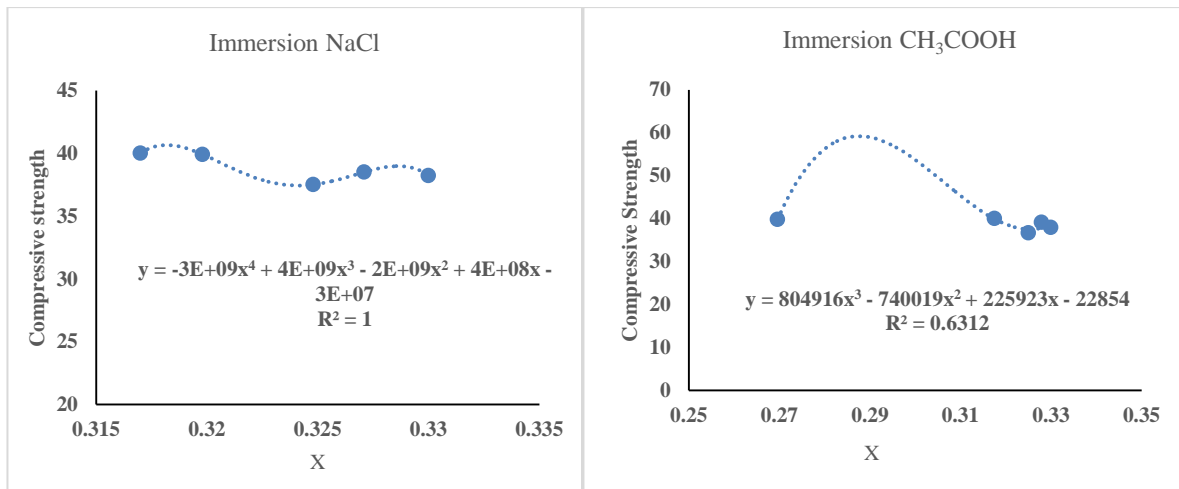


Figure 12. Polynomial curve fitting was employed to establish a correlation between chromaticity coordinates (x) and the corresponding compressive strengths of samples immersed in various reagents at a 5% concentration for 7, 14, 28, and 56 days.

8. Conclusion

1. Chromaticity diagrams and three-dimensional surface plots were utilised to examine the surface degradation brought on by soaking in hydrochloric acid, sulphuric acid, chloride of sodium, and acetic acid for seven, fourteen, twenty-eight, and fifty-six days. The results demonstrate that qualitative observations of colour changes in damaged surfaces can be effectively converted into quantitative data, facilitating mathematical analysis of colour variations.
2. For every form of immersion, chromaticity diagrams were created, and they showed generally uneven colour shifts from controlling cube data points. Notably, immersion in hydrochloric acid and sulfuric acid showed both red and white shifts, with changes becoming more pronounced up to 28 days. In contrast, immersion in sodium chloride and acetic acid exhibited more gradual shifts. The corresponding 3D surface plots of the damaged surfaces under these immersion conditions can be used to validate these findings.
3. Our study concludes that concrete is substantially deteriorated by sulphuric acid (H₂SO₄), with the most severe damage being evidenced by observable colour changes in M30 grade concrete that has been exposed to various chemicals. Acetic acid (CH₃COOH), while less potent than sulphuric acid, nonetheless had a discernible effect. Hydrochloric acid (HCl) and sodium chloride (NaCl) had the least impact on the concrete

samples. These findings emphasise the need of selecting appropriate materials and safety measures in environments where exposure to such potent chemicals is likely.

9. References

1. Guru Prathap Reddy, S., et al. (2020). *Correlation of Concrete Strength and Greyscale Intensity Under Acid Exposure*. Journal of Materials in Civil Engineering, 32(5), 04020037. Reference for correlation analysis of concrete strength and greyscale intensity.
2. Ostachowicz, W., & Güemes, A. (2013). *Structural Health Monitoring*. Wiley. Reference for sustainability in construction and degradation due to environmental factors.
3. Jurevicius, A., et al. (2014). *Digital Image Processing: Concepts and Applications*. Springer. Reference for the principles of digital image processing and its application in evaluating surface roughness and crack properties.
4. Redon, C., et al. (1999). *Studies on Fiber Orientation and Air Voids in Concrete*. Concrete Science and Engineering, 45(2), 123-137. Reference for investigations into fibre orientation and air voids in concrete.
5. Disquiet, J., et al. (2001). *Techniques for Measuring Air Void Distribution in Concrete*. Journal of Construction and Building Materials, 25(6), 789-798. Reference for methods to measure void distribution in concrete.
6. Dare, M., et al. (2002). *Automatic Feature Extraction for Crack Width Measurement*. Structural Engineering Review, 24(3), 345-359.

7. Reference for automatic algorithms for crack measurement. Valenca, J., et al. (2013). *Automated Crack Detection Systems*. Advanced Structural Engineering, 19(4), 467-478. Reference for advancements in automated systems for crack detection.
8. Kapur, J. N., et al. (1985). *Image Thresholding Techniques*. IEEE Transactions on Systems, Man, and Cybernetics, 15(6), 673-685. Reference for techniques in image thresholding and analysis.
9. Komac'ka, J., et al. (2019). *Standardizing Image Quality for Digital Processing*. Journal of Image and Graphics, 33(1), 12-24. Reference for factors affecting image quality in digital processing.
10. Yu, X., et al. (2019). *Threshold Selection Methodologies for Digital Images*. Computational Visual Media, 7(4), 457-469. Reference for methodologies in threshold selection for image processing.
11. Choi, Y., et al. (2017). *Techniques for Measuring Carbonation Depth in Concrete*. Journal of Civil Engineering and Management, 23(2), 263-275. Reference for methods to measure carbonation depth in concrete.
12. Ibraheem, A., et al. (2012). *Colour Space Models in Digital Image Processing*. Journal of Computational Imaging, 18(2), 147-160. Reference for different colour spaces used in digital image processing.
13. Panák, M., et al. (2018). *Enhancements in Colour Space Simulation for Thermochromic Samples*. Optical Engineering, 57(1), 011014. Reference for advancements in simulating human vision and colour perception.
14. Hasançebi, O., et al. (2010). *Artificial Neural Networks for Damage Detection in Structural Systems*. Structural Health Monitoring, 9(5), 47-62. Reference for the use of ANNs in structural damage detection.
15. Cheung, S., et al. (2004). *Colour Conversion Methods for Accurate Image Processing*. IEEE Transactions on Image Processing, 13(5), 612-621. Reference for methods to preserve colour fidelity during image processing.
16. Wei, X., et al. (2019). *Assessing Concrete Fire Damage Through Chromaticity Analysis*. Fire Safety Journal, 108, 85-94. Reference for assessing fire damage resistance in concrete using colour changes.
17. Mackechnie, J., & Alexander, M. (2009). *Durability Performance and Sustainability of Construction Materials*. Construction and Building Materials, 23(3), 1220-1229. Reference for evaluating durability performance and sustainability.
18. Press, R. (2007). *Impact of Degradation on Concrete Structures*. Journal of Building Performance, 4(2), 89-102. Reference for degradation effects on concrete and service life.
19. Basheer, P., et al. (2001). *Models for Assessing Concrete Durability*. Cement and Concrete Research, 31(8), 1245-1256. Reference for models and formulations for assessing concrete durability.